

Recipe of Polarized One-Electron Potential Optimization for Development of Polarizable Force Fields

Setsuko Nakagawa,^{*,†,‡} Pekka Mark,[‡] and Hans Ågren[‡]

Department of Human Life and Environment, Kinjo Gakuin University, Omori, Moriyama-ku, Nagoya 463-8521, Japan, and Department of Theoretical Chemistry, Royal Institute of Technology, S-106 91 Stockholm, Sweden

Received June 2, 2007

Abstract: Polarized one-electron potential (POP) optimization is a powerful and practical method to determine multicenter dipole polarizabilities that can be used for constructing polarizable force fields. The POP optimization is similar to the widely used electrostatic potential (ESP) optimization to determine the partial charges of molecules. However, while the ESP optimization targets the electrostatic potentials on a molecular surface, the POP optimization targets the change of electrostatic potentials on molecular surfaces which are induced by the field of a test charge on the molecular surface. Since only additional one-electron integrals for the test charge are required for the estimation of the surface potentials, the change of electrostatic potentials has been named “polarized one-electron potentials”. We show that in the POP optimization, both an explicitly interacting polarizability model and an implicitly interacting polarizability model can be used for the determination of the multicenter polarizabilities. In the explicitly interacting model, intramolecular induced dipole–induced dipole interaction is mutually included in the process of the POP optimization, but the interaction is not included in the implicitly interacting model. In the implicitly interacting polarizability model, a combined model of isotropic atom polarization and anisotropic bond polarization is shown to provide the best fitting results for nucleic acid bases which show large polarization anisotropy. A simple scaling model to the chemical bond has been newly proposed for the explicitly interacting polarizability model. We show that the simple model can be applied to molecular simulations without any damping of exponential type in the intramolecular induced dipole interaction. A detailed procedure for determination of the multicenter dipole polarizability by the POP optimization is also presented.

Introduction

Classical molecular simulations constitute an indispensable tool in theoretical studies of biomolecular systems such as proteins, nucleic acids, and membranes as well as physico-chemical systems.^{1–7} Molecular mechanics (MM) force fields are commonly used for molecular dynamics simulations to investigate dynamical structures and thermodynamical properties of the biomolecular systems.^{8–11} Nowadays MM and

quantum mechanics (QM) methods are often combined, QM/MM,^{12–14} as a significant tool to study reaction mechanisms of enzymes. So far additive two-body potential functions have been mainly used in the MM force fields for biomolecular systems. The gap of potential quality between the QM and MM is, however, still quite large. Although the average polarization taking place in the condensed phase is included, the two-body potential does not respond to the electron density redistribution due to the ambient electric field. Potential functions that respond to a nonhomogeneous environment such as biomolecular systems can be made by the explicit inclusion of polarization. Computationally, the

* Corresponding author fax: +81 52 798 0370; e-mail: naka@kinjo-u.ac.jp.

[†] Kinjo Gakuin University.

[‡] Royal Institute of Technology.

implementation of a polarizable force field that adds a polarization term to the existing two-body potential is becoming a realistic proposition as the operation speed and memory capacity of the computers are much improved. This fact has indeed advanced the development of the polarizable force fields for biomolecular systems.^{15–24}

The response of a molecule to an external polarizing field is essentially nonlocal, and the multicenter polarizabilities are not observable physical quantities. Until now, several polarization models have been reported. They can be classified in polarization models of two principal types,²⁵ namely as an explicitly interacting polarizability model and an implicitly interacting polarizability model. In the explicitly interacting model, intramolecular induced dipole–induced dipole interaction is included directly, but the intramolecular interaction is not included in the implicitly interacting model. The former model has been proposed, for instance, from an empirical method that is a simple approximation for predicting and rationalizing average molecular polarizabilities.^{26–29} The latter model has been studied using quantum mechanics as distributed polarizabilities.³⁰

An inducible point dipole (PD) model where the induced dipole–induced dipole interaction in the molecule is explicitly included has often been used for the polarizable force fields. The interacting atomic dipole model by Applequist et al. was employed in the AMBER/ff02 force field.^{16,17} The intramolecular fields will be severely damped if they are included. In their approach the intramolecular electric fields from atoms separated by one and two chemical bonds were excluded. Thole improved the interacting atomic dipole model by introducing the modification of a dipole field tensor.²⁷ The predicted anisotropy of molecules was significantly improved by the modification. One of the damping models was employed for the AMOEBA polarizable force field.^{18,19} Furthermore, a classical Drude oscillator model has been proposed, that is a variation of the PD model. Each polarizable atom is then represented by a pair of point charges of opposite sign bound by a stiff spring. This model with the short-range damping was employed in the CHARMM program.²³ Because very large force constants are used for the bonds between each atom and its Drude particle, the Drude particle stays close to the atom. The Drude model gives almost the same calculation result as the inducible PD model in the numerical value.

The microscopic electronic response of polarization has been studied using quantum mechanical calculations. It is noted that the intramolecular polarization is included implicitly at the QM level. The induced dipoles represent directly the electron cloud that changes by an external electric field. Accordingly, the induced dipoles can be simply added in the implicitly interacting polarizability models. The distribution of molecular polarizability which is estimated from the QM calculation has been studied based on a general theory developed by Stone.³⁰ Jansen et al. presented a robust scheme to calculate the distributed polarizabilities and distributed multipoles based on the partitioning of the physical space into atomic regions.³¹ However, this scheme encountered difficulties for use in MM calculations, because of the manifold of parameters that have to be included. The

dipole molecular polarization was distributed approximately on the centroids of localized orbitals by Gammer and Stevens.³² Such distributed polarizabilities have been adopted in the SIBFA polarizable mechanics procedure.²⁴

The fluctuating charge (FQ) model, where the principle of electronegativity equalization is used, is also categorized as the implicitly interacting model. This model has been adopted for the polarizable force field for proteins.²² The FQ model may be computationally the most efficient model, but as this model has limitations in the spatial distribution of induced charges it has been combined with the PD model.²⁰

A quite powerful and practical method to determine the multicenter polarizabilities was proposed in 1993.³³ In this method, first, the changes of electrostatic potentials mapped on a molecular surface induced by an external electric field point charge (test charge) are estimated using a QM method. A series of potential maps changed by a test charge put on an appropriate molecular surface is then required. Next, the multicenter polarizabilities are optimized in order to reproduce the surface potentials derived from the QM calculations. The change of electrostatic potentials is named polarized one-electron potentials (POP), because additional one-electron integrals are required by a test charge. In this methodology, the POP optimization is similar to electrostatic potential (ESP) optimization that is widely used to determine the partial charges of molecules.³⁴ While the ESP optimization targets the electrostatic potentials on the molecular surface, the POP optimization targets the change of electrostatic potentials on this surface. The POP optimization is applicable to both of the explicitly interacting model and the implicitly interacting model.

The POP optimization method was first applied for a water molecule.³³ Subsequently the anisotropic contribution of polarization and the transferability of multicenter polarizabilities were studied.^{35,36} Two models of the isotropic atom polarization and the anisotropic polarization along the chemical bond (anisotropic bond polarization) were employed, and it was shown that the combination of the isotropic and anisotropic polarization brings good results in the POP optimization. This resembles the combination of FQ and PD.²⁰ The polarized model potential (PMP) function composed of Coulomb, van der Waals, and polarization terms was constructed for methanol and nucleic acid bases based on the parameters derived from the ESP and POP optimization methods.^{37,38} The potential energy surfaces estimated using high-level *ab initio* molecular orbital (MO) calculations were reproduced quite well by the PMP function.

Ángyán et al. proceeded detailed studies and presented a formulation for distributed multipoles.³⁹ In their method, the energies induced by a test charge are mapped for the target of optimization instead of POP. The similar optimization method using surface POP was independently developed by Kaminski et al.²⁰ They used a dipolar probe which mimics liquid water instead of a single test charge. Recently, the polarization parameters of Drude particles and atomic charges were derived by the surface potential optimization method using a test charge.²³ Thus, the optimization that uses the test charge(s) has become a standard method to obtain a

variety of polarization parameters from the QM calculations. However, since the high-level QM calculations are still time-consuming for larger molecules, the polarization model and the polarizability parameters have not yet been fully developed.

In this study, the explicit and implicit interacting polarizability models are investigated by using the POP optimization. Four nucleic acid bases which were used in the previous work³⁸ are studied further. As the nucleic acid bases show large polarization anisotropy, they are good model molecules for this research. The aim of this work is to assess the polarization models and to offer a protocol of the POP optimization for development of polarizable force fields.

Method

Electrostatic Potential Optimization and Polarized One-Electron Potential Optimization. Electrostatic potential optimization has been used as a practical method to determine partial charges of molecules.³⁴ The electrostatic potentials at several points (\mathbf{R}_l) on an appropriate molecular surface are evaluated from the wave function of an isolated molecule and are used as the reference of the charge optimization. The electrostatic potential is rigorously defined by the quantum mechanical expression

$$V^{\text{QM}}(\mathbf{R}_l) = \sum_i \frac{Z_i}{|\mathbf{R}_l - \mathbf{R}_i|} - \int \frac{\rho(\mathbf{r})}{|\mathbf{R}_l - \mathbf{r}|} d\mathbf{r} \quad (1)$$

Here the first term represents the electrostatic contribution from the nuclear charges Z_i located at positions \mathbf{R}_i , and the second term represents the electrostatic potential originating from the electron density $\rho(\mathbf{r})$ throughout the whole space. In the evaluation of the electrostatic potential the wave function of the unperturbed Hamiltonian (H_0) is kept frozen (ϕ_0) under perturbation.

In the classical picture, the electron density is approximated by discrete point charges (q_i). The classical electrostatic potential given as

$$V^{\text{CM}}(\mathbf{R}_l) = \sum_i \frac{q_i}{|\mathbf{R}_l - \mathbf{R}_i|} \quad (2)$$

is estimated on the same molecular surface. The Levenberg–Marquardt nonlinear optimization procedure⁴⁰ is used to minimize the following target function in order to determine the fractional point charges:

$$\chi^2 = \sum_l^L [V^{\text{CM}}(\mathbf{R}_l) - V^{\text{QM}}(\mathbf{R}_l)]^2 \quad (3)$$

The polarized one-electron potential optimization method is used to determine the multicenter polarizabilities.^{33,35,36} In this methodology, the POP optimization is similar to the ESP optimization. To evaluate the polarization effect, it is necessary to relax the wave function (ϕ_k) under the perturbed Hamiltonian ($H_0 + H_k$). Here, a molecule is perturbed by an external electric field test charge (q_k). When the molecule is polarized, the one-electron potential is modified. In quantum mechanics, we can evaluate the change in the one-

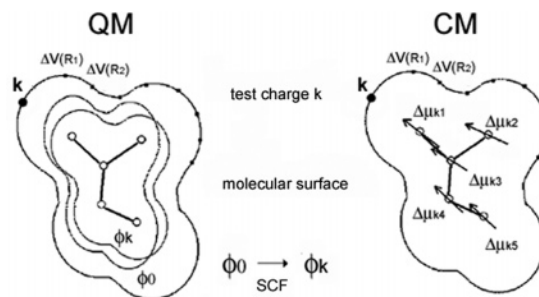


Figure 1. Schematic representation of POP optimization.

electron potential ($\Delta V_k^{\text{QM}}(\mathbf{R}_l)$) by the polarization as follows:

$$\Delta V_k^{\text{QM}}(\mathbf{R}_l) = \int \frac{\Delta \rho_k(\mathbf{r})}{|\mathbf{R}_l - \mathbf{r}|} d\mathbf{r} \quad (4)$$

Here $\Delta \rho_k(\mathbf{r})$ is the difference between the electron densities obtained from the frozen and relaxed wave functions (ϕ_0 and ϕ_k). Since only one-electron integrals for the test charge are required for the estimation of the surface potentials of ϕ_k , the change of electrostatic potentials was named polarized one-electron potentials. The QM calculation with the test charge is the most time-consuming step, because it requires large sets of points to sample the space around the molecule appropriately. However, the two electron integrals can be reused repeatedly. This was a useful method in the age when the operation speed of the computer was not too fast.

On the other hand, in the classical picture the difference is approximated as several discrete fractional charges (Δq_{ki}) as follows:

$$\Delta V_k^{\text{CM}}(\mathbf{R}_l) = \sum_i \frac{\Delta q_{ki}}{|\mathbf{R}_l - \mathbf{r}_i|} \quad (5)$$

Since the sum of the discrete charges should be zero, an induced dipole model is introduced. The inducible point dipoles, the fluctuating charges, and the Drude oscillator models can be treated for the discrete fractional charges. Here, isotropic atom induced dipoles (induced charges of $-\Delta q^a$ and $+\Delta q^a$) and/or anisotropic bond induced dipoles (induced charges of $-\Delta q^b$ and $+\Delta q^b$) are used for the implicitly interacting polarization model. In Figure 1, the schematic representation of the POP optimization for the isotropic atom induced dipole model is presented. For the explicitly interacting model inducible point dipoles ($\Delta \mu^l$) are used.

The nonlinear optimization procedure⁴⁰ is used to minimize the following quantity in order to determine the induced dipoles:

$$\chi^2 = \sum_j^J \sum_k^K \sum_l^L [\Delta V_{jk}^{\text{CM}}(\mathbf{R}_l) - \Delta V_{jk}^{\text{QM}}(\mathbf{R}_l)]^2 \quad (6)$$

Here, j and k are the strength and position of the test charge, respectively. A test charge is placed on the molecular surface defined by an envelope of 1.8 times the van der Waals radius of the atoms when not specified, and test charges of -0.5 e and $+0.5$ e are used ($J = 2$) unless specified.

The multicenter polarizabilities of the nucleic acid bases are optimized to reproduce the polarized one-electron potentials obtained from the MP2/6-31+G* wave function.^{41–43} The geometries of the nucleic acid bases are optimized at the MP2/6-31G** level. The numbers of test charge places (K) of adenine, cytosine, guanine, and thymine are 222, 194, 229, and 226, respectively. These numbers are the same as in the previous work.³⁸ The one-electron potential change by the polarization is estimated on the same positions of test charges. The number of the estimated points (L) was equally taken with K though neither K nor L had necessarily to be the same. In the example of adenine, the POP data of $2 \times 222 \times 222$ points were used for the fitting.

Implicitly and Explicitly Interacting Polarizability Models. The locally induced dipoles are used for the discrete charges. Since the intramolecular polarization is included at the quantum mechanical level, a simple polarization model to respond to the test charge can be used. This model is an implicitly interacting induced charge model. Two types of the induced dipoles are considered: an isotropic atom induced dipole ($\Delta\mu_{km}^a$) and an anisotropic bond induced dipole ($\Delta\mu_{km}^b$). The former shows a spatial movement of the charges around the atom, and the latter shows the movement of the charges along the chemical bond. The polarization anisotropy of the molecule can be introduced in the bond polarizabilities more clearly though the molecular anisotropy can be shown to some degree by the isotropic atom polarization. The induced dipoles are expanded by power series of the electric fields (\mathbf{F}_{km}) at the centers (m) of the dipoles, which are produced by the test charge. Here, the higher order terms are truncated, because the energetic contribution of the hyperpolarizability is expected to be small in the molecular interactions treated here. The induced dipoles are defined as

$$\Delta\mu_{km}^a = \Delta q_{km}^a \mathbf{r}_{m_1} - \Delta q_{km}^a \mathbf{r}_{m_2} \approx \alpha_m^a \mathbf{F}_{km} \quad (7)$$

$$\Delta\mu_{km}^b = \Delta q_{km}^b \mathbf{r}_{m_a} - \Delta q_{km}^b \mathbf{r}_{m_b} \approx \alpha_m^b (\mathbf{F}_{km} \cos \theta_{km}) \quad (8)$$

where Δq_{km}^a and Δq_{km}^b are the induced charges representing the isotropic atom and anisotropic bond induced dipoles, respectively, and \mathbf{r}_{m_1} , \mathbf{r}_{m_2} , \mathbf{r}_{m_a} , and \mathbf{r}_{m_b} are the positional vectors of the locally induced dipole. α denotes the multicenter polarizability, and θ_{km} is an angle between the electric field vector and the chemical bond direction. α is the optimization parameters of eq 6. Because the treatment of the isotropic atom dipoles and the anisotropic bond dipoles does not need the setting of local coordinates, the handling is easy in the MM calculation. For the isotropic atom induced dipole moments, $|\mathbf{r}_{m_1} - \mathbf{r}_{m_2}|$ is set to 1.0 bohr. Because the induced dipole of 1.0 bohr is sufficiently buried in the van der Waals surface of the molecule, the spatial movement of the charges can be expressed well. For the anisotropic bond induced dipoles the induced charges are placed on the atoms of the bond. Because the treatment of adding the induced charge to the atomic charge is possible, the calculational efficiency can be improved in the MM calculations. The models using the isotropic atom and anisotropic bond induced dipoles are called model a and model b, respectively. The combined model is called model ab here.

An explicitly interacting polarizability model is also used for the POP optimization, namely the atom dipole interaction model proposed empirically by Applequist et al. in order to determine atomic polarizabilities from a set of experimental molecular polarizabilities.²⁶ The atoms are here regarded as isotropically polarizable points located at their nuclei, interacting via the fields of their induced dipoles. The induced dipole is given by using test charge field (\mathbf{F}_{km}) as

$$\Delta\mu_{km}^I = \alpha_m^I [\mathbf{F}_{km} - \sum_{n \neq m}^N \tilde{\mathbf{T}}_{mn} \Delta\mu_n^I] \quad (9)$$

where $\tilde{\mathbf{T}}_{mn}$ is the dipole field tensor and $\Delta\mu_n^I$ is the induced dipole moment in the molecule. This model is called model A here.

We also employed Thole's modification of the intramolecular dipole interaction for repairing the deficiency of infinite polarization by the cooperative interaction between two induced dipoles in the direction of the line connecting the two.²⁷ The dipole field tensor is modified using the damping coefficients (λ_3 and λ_5) as follows

$$\tilde{\mathbf{T}}_{mn} = \lambda_3 \frac{\tilde{\mathbf{I}}}{r_{mn}^3} - 3\lambda_5 \frac{\mathbf{r}_{mn} \otimes \mathbf{r}_{mn}}{r_{mn}^5} \quad (10)$$

where $\tilde{\mathbf{I}}$ is the unit tensor, r_{mn} is the distance between atoms m and n , and \mathbf{r}_{mn} is the vector connecting atoms m and n . Various forms of the modification which is related to a charge distribution were investigated by Thole.²⁷ Van Duijnen and Swart investigated further the linear and exponential type dampings.²⁸ The forms of the exponential type damping are

$$\lambda_3 = 1 - \left(\frac{a^2 u^2}{2} + au + 1 \right) \exp(-au) \quad (11)$$

$$\lambda_5 = 1 - \left(\frac{a^3 u^3}{6} + \frac{a^2 u^2}{2} + au + 1 \right) \exp(-au) \quad (12)$$

where u is $r_{mn}/(\alpha_m \alpha_n)^{1/6}$, and a is the damping factor (1.9088). This is called model T with the damping type Exp 1 (model T1).

Ren and Ponder adopted different damping forms in their AMOEBA polarizable force field as follows:^{18,19}

$$\lambda_3 = 1 - \exp(-au^3) \quad (13)$$

$$\lambda_5 = 1 - (au^3 + 1) \exp(-au^3) \quad (14)$$

They assigned 0.39 as the damping factor. This model is called model T with damping type Exp 2 (model T2).

A new damping model is tested here. In the molecular mechanics calculations, electrostatic interactions of atoms separated by one bond (1–2) and by two bonds (1–3) are always neglected. The electrostatic interactions of atoms separated by three bonds (1–4) are usually scaled by 0.5. In the same way the dipole field tensor $\tilde{\mathbf{T}}_{mn}$ is simply scaled. This model is called model S. The best scaling factors are investigated here.

We also consider the Drude oscillator model used in the CHARMM program in order to incorporate the polarizable

force field.²³ The dipole field tensor is then scaled using the following factor

$$S_{mn} = 1 - \left(\frac{au}{2} + 1\right) \exp(-au) \quad (15)$$

where a is 2.6. The scaling is applied for the 1–2 and 1–3 induced dipole–induced dipole interaction. This model is called model D with the damping type Exp 3 (model D3). The force constant of the atom-Drude bonds is 1000 kcal/mol/Å².

The effects of permanent dipoles (or permanent charges) in the molecule can be omitted as pointed out by Applequist et al. since these do not affect the net moment induced by an external field.²⁶ However, in the development of polarizable force fields for relatively large molecules such as proteins and DNA, a consistent treatment for inter- and intramolecular polarizations might be required for induced dipole-permanent charge interactions. The intramolecular induced dipole-permanent charge interaction is studied for nucleic acid bases using the simple scaling such as model S.

Evaluation of POP, Induction Energy, and Induced Dipole Moment. In order to evaluate the polarization model and the intramolecular damping, the root-mean-square deviations (rmsd) of POP is estimated as

$$\text{rmsdPOP} = \sqrt{\frac{\sum_j^J \sum_k^K \sum_l^L [\Delta V_{jk}^{\text{CM}}(\mathbf{R}_l) - \Delta V_{jk}^{\text{QM}}(\mathbf{R}_l)]^2}{JKL}} \quad (16)$$

The relative rms deviation (rrmsd) of POP from the QM values is also estimated as the percentage.

The induction (polarization) energies are used for the evaluation of the models. In quantum mechanics the induction energy (IE) is given as

$$\Delta U_k^{\text{QM}} = \langle \phi_k | H_0 + H_k | \phi_k \rangle - \langle \phi_0 | H_0 + H_k | \phi_0 \rangle = E_k - E_0 - q_k V_k^{\text{QM}} \quad (17)$$

where E_k and E_0 are the total energies of the molecule in the presence and in the absence of the test charge, respectively. V_k^{QM} is the electrostatic potential at point k of the molecule without the test charge. In classical mechanics the induction energy of the isotropic induced dipoles is given as

$$\Delta U_{jk}^{\text{CM}} = -\frac{1}{2} \sum_m \Delta \mu_m \mathbf{F}_m^{jk} \quad (18)$$

The root-mean-square deviation of the induction energies is computed as

$$\text{rmsdIE} = \sqrt{\frac{\sum_j^J \sum_k^K (\Delta U_{jk}^{\text{CM}} - \Delta U_{jk}^{\text{QM}})^2}{JK}} \quad (19)$$

The relative rms deviation of the induction energy from the QM values is also estimated. In the study of optimally partitioned electric properties (OPEP) by Ángyán et al. these

induction energies are mapped for the target of optimization instead of POP.^{25,39}

The induced dipole moments of the molecule are also used for the evaluation of the models. The QM induced dipole moment of molecule is given as follows

$$\Delta \mu_{jk}^{\text{QM}} = \mu^{jk} - \mu^0 \quad (20)$$

where μ^{jk} and μ^0 are the dipole moments of the molecule in the presence and in the absence of the test charge, respectively, while in classical mechanics the induced dipole moment of molecule is given as

$$\Delta \mu_{jk}^{\text{CM}} = \sum_m \Delta \mu_m^{jk} \quad (21)$$

The root-mean-square deviation of the induced dipole moments is computed as

$$\text{rmsdIDM} = \sqrt{\frac{\sum_j^J \sum_k^K (\Delta \mu_{jk}^{\text{CM}} - \Delta \mu_{jk}^{\text{QM}})^2}{JK}} \quad (22)$$

Intermolecular Interaction of the Polarizable Model Potential Function. The optimized multicenter polarizabilities are applied for the estimation of the interaction energies of the nucleic acid base pairs. The polarizable model potential (PMP) function which consists of a electrostatic term (E_{es}), a van der Waals term (E_{vdw}), and a polarization term (E_{plz}) is used for the estimation of the total energy (E_{PMP}) of an interacting molecular system.³⁷

$$E_{\text{PMP}} = E_{\text{es}} + E_{\text{vdw}} + E_{\text{plz}} \quad (23)$$

The electrostatic energy is represented by the Coulomb form using the permanent partial charges of the molecules. The charges were optimized by the ESP optimization. The van der Waals (vdw) interactions are represented by the Lennard-Jones potential. The intramolecular charge–charge and the intramolecular vdw interactions are not taken into account in the energy because they are canceled in the rigid structure. The charge and vdw parameters of the nucleic acid bases are taken from the previous work.³⁸

The polarization energy is expressed as

$$E_{\text{plz}} = -\frac{1}{2} \sum_i^N \Delta \mu_i \mathbf{F}_i^0 \quad (24)$$

Here, $\Delta \mu_i$ is the induced dipole moment of site i , and \mathbf{F}_i^0 is the electrostatic field at site i due to the permanent charges of all other sites belonging to different molecules. The induced dipole moments are calculated self-consistently as follows:

$$\Delta \mu_i = \alpha_i (\mathbf{F}_i^0 - \sum_j \tilde{\mathbf{T}}_{ij} \Delta \mu_j) \quad (25)$$

Here, α_i is the polarizability of site i . In the implicitly interacting polarizability model, site j is not in the molecule containing site i . The intramolecular polarizations of induced dipole–induced dipole and the intramolecular polarization

of induced dipole-permanent charge are not taken into account. In the explicitly interacting polarizability model the intramolecular induced dipole–induced dipole polarization is taken into account according to the damping type. In the present work the intramolecular polarization of induced dipole-permanent charge is not taken into account unless specified. The dipole field tensor is given as follows:

$$\tilde{\mathbf{T}}_{ij} = \frac{\tilde{\mathbf{I}}}{r_{ij}^3} - \frac{3\mathbf{r}_{ij} \otimes \mathbf{r}_{ij}}{r_{ij}^5} \quad (26)$$

For the induced dipole–induced dipole damping the following consistent formula for intra- and intermolecular interaction can be used.

$$\tilde{\mathbf{T}}_{ij} = \lambda_3 \frac{\tilde{\mathbf{I}}}{r_{ij}^3} - 3\lambda_5 \frac{\mathbf{r}_{ij} \otimes \mathbf{r}_{ij}}{r_{ij}^5} \quad (27)$$

An iterative procedure is used to solve eq 25. Convergence is achieved when the deviation of the induced dipole moments from two sequential iterations falls to within 0.00025 Debye/site.

Evaluation of Surface Electrostatic Potentials of Complex Molecules. The surface electrostatic potential of a complex molecule is calculated from the nuclear charge Z_i and the electron density $\rho(\mathbf{r})$ as follows:

$$V^{\text{QM}}(\mathbf{R}_l) = \sum_i \frac{Z_i}{|\mathbf{R}_l - \mathbf{R}_i|} - \int \frac{\rho(\mathbf{r})}{|\mathbf{R}_l - \mathbf{r}|} d\mathbf{r} \quad (28)$$

Here, the complex molecule AB is treated as a supermolecule. The surface potential for complex molecule using the PMP function is calculated from atomic charges and induced dipoles as follows

$$V^{\text{PMP}}(\mathbf{R}_l) = \sum_i \frac{q_i}{|\mathbf{R}_l - \mathbf{r}_i|} - \sum_j \frac{\Delta\mu_j \cos\theta_j}{|\mathbf{R}_l - \mathbf{r}_j|} \quad (29)$$

where θ_j is an angle between the vector $\mathbf{R}_l - \mathbf{r}_j$ and the induced dipole vector $\Delta\mu_j$. The rms deviation of the electrostatic potentials is given by

$$\text{rmsdESP} = \sqrt{\frac{\sum_l^L [V^{\text{PMP}}(\mathbf{R}_l) - V^{\text{QM}}(\mathbf{R}_l)]^2}{L}} \quad (30)$$

The relative rms deviation of ESP from the QM values is estimated as the percentage.

All of the ab initio MO calculations are done with the Gaussian03 computer program.⁴³

Results

Polarization Models. Using the implicitly interacting polarizability model and the explicitly interacting polarizability model, the multicenter polarizabilities of four nucleic acid bases were determined by POP optimization. MP2/6-31+G* was used for the calculations of polarized one-electron potentials on the molecular surfaces, because this approach gave molecular polarizabilities relatively close to the ex-

Table 1. Root-Mean-Square Deviation of Polarized One-Electron Potentials in kcal/mol, Induction Energies in kcal/mol, and Induced Dipole Moments in Debye of Various Polarization Models for Four Nucleic Acid Bases

model	damping type	molecule	rmsd (rmsd %)		
			POP	IE	IDM
a		A	1.4 (31)	0.4 (15)	0.6 (19)
		T	1.2 (29)	0.3 (14)	0.5 (11)
		C	1.3 (32)	0.4 (14)	0.6 (8)
		G	1.4 (32)	0.4 (16)	0.7 (9)
b		A	1.6 (36)	1.0 (34)	0.6 (20)
		T	1.0 (29)	0.7 (27)	0.5 (10)
		C	1.4 (34)	0.8 (33)	0.6 (8)
		G	1.4 (33)	0.8 (31)	0.6 (9)
ab		A	0.6 (13)	0.3 (11)	0.2 (5)
		T	0.4 (9)	0.2 (8)	0.1 (2)
		C	0.5 (12)	0.3 (10)	0.2 (3)
		G	0.5 (12)	0.3 (11)	0.2 (2)
A		A	1.2 (27)	0.9 (32)	0.4 (12)
		T	0.8 (20)	0.6 (23)	0.2 (5)
		C	1.0 (24)	0.8 (29)	0.3 (4)
		G	1.1 (25)	0.8 (29)	0.4 (5)
T1	Exp 1	A	0.6 (13)	0.3 (10)	0.2 (7)
		T	0.5 (12)	0.2 (8)	0.2 (4)
		C	0.5 (12)	0.2 (9)	0.2 (2)
		G	0.5 (13)	0.3 (10)	0.2 (3)
T2	Exp 2	A	0.7 (15)	0.4 (13)	0.3 (8)
		T	0.7 (17)	0.3 (14)	0.3 (6)
		C	0.9 (20)	0.5 (18)	0.3 (4)
		G	0.7 (17)	0.4 (14)	0.3 (4)
D3	1-2,1-3 Exp 3	A	1.1 (25)	0.4 (14)	0.5 (15)
		T	1.0 (26)	0.3 (12)	0.5 (9)
		C	1.2 (28)	0.3 (13)	0.5 (7)
		G	0.6 (15)	0.3 (10)	0.3 (4)
S	1-2 0.1	A	0.5 (11)	0.3 (12)	0.1 (4)
		T	0.5 (13)	0.2 (9)	0.2 (4)
		C	0.5 (12)	0.3 (11)	0.2 (2)
		G	0.5 (10)	0.3 (11)	0.1 (2)

perimental values in solution as shown in the previous study.³⁸ The polarization reduction by the exchange repulsion in the condensed phase might be taken into account by this basis set.

The root-mean-square deviations of polarized one-electron potentials, induction energies, and induced dipole moments of various polarization models for the four nucleic acid bases are shown in Table 1. In the implicitly interacting induced charge model, model ab shows the best results in the POP fitting. The relative rms deviations of model ab are 9–13%. The rms deviation of induction energies and induced dipole moments were only 8–11% and 2–5%, respectively. These IE and IDM results estimated from the optimized induced charges showed better results compared with the results of POP that inspected the electronic density change in detail. The model ab has shown quite good results for acetylene, ethylene, and benzene.³⁵ The combination of isotropic induced dipoles at atom centers with anisotropic induced dipoles along bonds is significant for describing the molecular polarization with large anisotropy.

Table 2. Multicenter Polarizability in au of Implicitly Interacting Induced Dipole Models

model	molecule	isotropic atom polarizability (au)				anisotropic bond polarizability (au)				
		C	N	H	O	C–C	C–H	C–N	N–H	C–O
a	A	4.555	10.122	1.983						
	T	6.614	5.502	2.121	6.983					
	C	7.688	6.004	2.354	7.576					
	G	6.532	7.600	1.891	7.689					
b	A					23.61	10.37	18.87	5.96	
	T					19.03	8.93	14.32	7.02	23.40
	C					19.01	5.35	21.43	4.80	22.08
	G					10.01	6.31	21.05	4.48	23.82
ab	A	0.464	9.047	0.762		15.88	5.73	9.50	−0.46	
	T	9.853	0.866	3.025	13.279	9.85	3.02	10.18	0.87	13.28
	C	4.272	3.850	1.718	3.850	10.07	0.58	12.67	−0.16	13.92
	G	2.268	5.693	1.177	5.781	8.63	3.51	11.34	−0.41	11.63
additive (empirical) ^a		6.93	8.34	2.75	5.68					

^a The atomic polarizabilities of C (alkane), N (nitrile), H (alkane), and O (carbonyl) are shown.²⁶

Model A, which is the explicitly interacting polarizability model without damping, shows better results in comparison with the additive model (model a) in the POP fitting. However, the induction energies were overestimated. In the explicitly interacting model, model T1 and model S show significantly similar results compared to model ab in the POP fitting. The results of model S are the best ones when scaling 0.1 is given to the 1–2 bonds. The results of model T2 and model D3 are somewhat worse.

The optimized polarizabilities of the implicitly interacting polarization model are shown in Table 2. The parameters of each atomic species have been optimized in model a. H, C, N, and O polarizability parameters of four nucleic acid bases were almost converged, though the values C and N of adenine depart somewhat. Similar convergence was found for alkanes and alcohols in the POP optimization.³⁶ The parameters of model a can be compared with the empirical values of the additive model listed by Applequist.²⁶

The optimized polarizabilities of the explicitly interacting polarization model are shown in Table 3. The parameters of each atomic species have been optimized. The atomic polarizabilities of model A are smaller than those of model a, since the mutual induction enhances the molecular polarizability in model A. The convergence of parameters is relatively good in models A and S. The atomic polarizabilities changed according to the type of the damping.

Condition of POP Optimization. Since the results of model S were good in the explicitly interacting polarizability model though the damping form was quite simple, further investigations were performed using this model. In the first paper on the POP optimization we investigated the strength of field point charges using water molecule.³³ It was shown that the polarizabilities are changed exponentially and that the deviations are greatly increased in the highly positive field. In Figure 2 the effects of a field test charge for guanine are shown. The optimized polarizabilities are almost constant from −1.5 e to +0.5 e. However, they change rapidly when +1.0 e is exceeded. In the region between −1.0 e and +0.5 e the rms deviation of POP is less than 11% but increases to 26% for +1.0 e. In this study simultaneous fittings were performed using −0.5 e and +0.5 e leading to good results

Table 3. Atomic Polarizability in au of Explicitly Interacting Induced Dipole Models

			atomic polarizability (au)			
model	damping type	molecule	C	N	H	O
A		A	4.759	3.417	0.736	
		T	4.325	3.235	1.107	3.021
		C	4.511	3.566	0.764	2.932
		G	4.905	3.133	0.827	2.158
T1	Exp 1	A	7.937	11.967	0.756	
		T	10.379	7.331	1.278	7.711
		C	11.986	9.674	0.718	7.703
		G	8.265	11.027	0.531	8.671
T2	Exp 2	A	2.022	15.488	1.959	
		T	4.388	10.690	3.375	9.572
		C	3.531	14.401	2.625	9.345
		G	1.815	14.632	1.632	10.626
D3	1-2,1-3 Exp 3	A	2.136	13.367	1.650	
		T	5.883	5.424	2.614	7.848
		C	7.295	5.611	2.917	8.163
		G	7.714	7.494	1.222	7.275
S	1-2 0.1	A	6.654	8.302	0.992	
		T	7.308	5.202	1.440	7.221
		C	8.316	6.945	1.029	6.834
		G	6.854	7.493	0.901	7.588
empirical						
A ^a			6.93	8.34	2.73	5.68
T ^b Exp 1			8.794	6.670	3.059	5.648

^a The atomic polarizabilities of C (alkane), N (nitrile), H (alkane), and O (carbonyl) are shown.²⁷ ^b Atomic polarizabilities fitted to the original 16 molecules.²⁸

(10%) as shown in Table 1. Very similar results were obtained using the test charge of +0.1 e as shown in Figure 2. To reduce computational time the single test charge of +0.1 e might be a good choice.

The effect of the van der Waals surface in which the test charge was located was investigated. Here, the same surface points were used to evaluate the polarized one-electron potentials. The single test charge of +0.1 e was used. In Figure 3 the changes in atomic polarizabilities are plotted for the vdw radius of the atoms. The almost constant atomic polarizabilities were obtained in the region from 1.6 to 3.0 times the vdw radius of atoms. The rms deviations are less

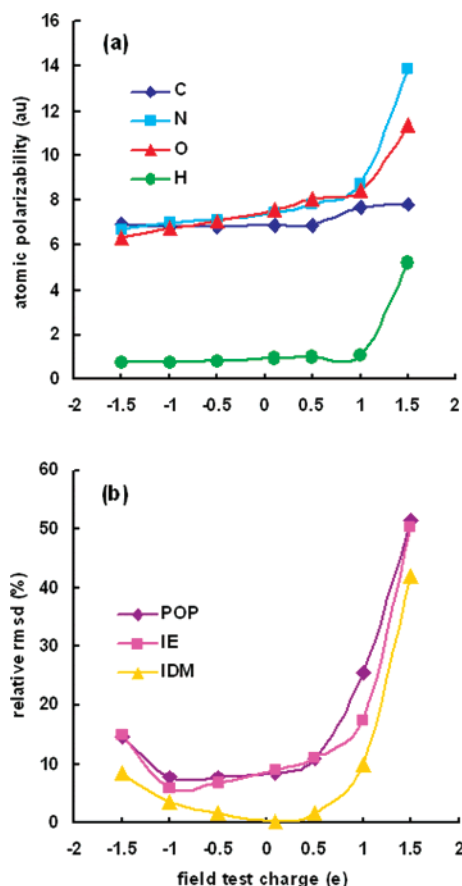


Figure 2. (a) Variations of atomic polarizabilities of guanine for field test charges. (b) Relative root-mean-square deviations of polarized one-electron potential fitting, induction energies, and induced dipole moments.

than 10%. The POP optimization did not succeed at the surface of the 1.4 times of the vdw radius, because of the penetration of the test charge to the electron cloud. So far we have used the 1.8 times the vdw radius. This single surface choice is reasonable.

Simple Scaling Model. The scaling effect for the induced dipole-induced dipole interactions was studied in detail using model S of guanine. The effect of atoms separated by one bond (1–2) is shown in Figure 4. The atomic polarizabilities changed greatly by the scaling. The best result of the POP optimization was obtained with the scaling of 0.1–0.2. The best result of induction energy was obtained in the scaling of 0.0. Thus, it is necessary to scale down the induced dipole-induced dipole interactions between atoms making the chemical bonds.

The effect of atoms separated by two bonds (1–3) is shown in Figure 5. Here, the 1–2 interaction has been scaled by zero. The changes of atomic polarizabilities are found to be quite minor. The best result of the POP optimization was obtained for the scaling of 1.0. A complete inclusion of the 1–3 interaction is necessary contrary to the 1–2 interaction. Moreover, a complete inclusion of the 1–4 interaction or more improves somewhat the rms deviation. Thus, model S in which the 1–2 interactions are scaled by 0.1 works well. In the linear model of Thole atoms separated by two bonds

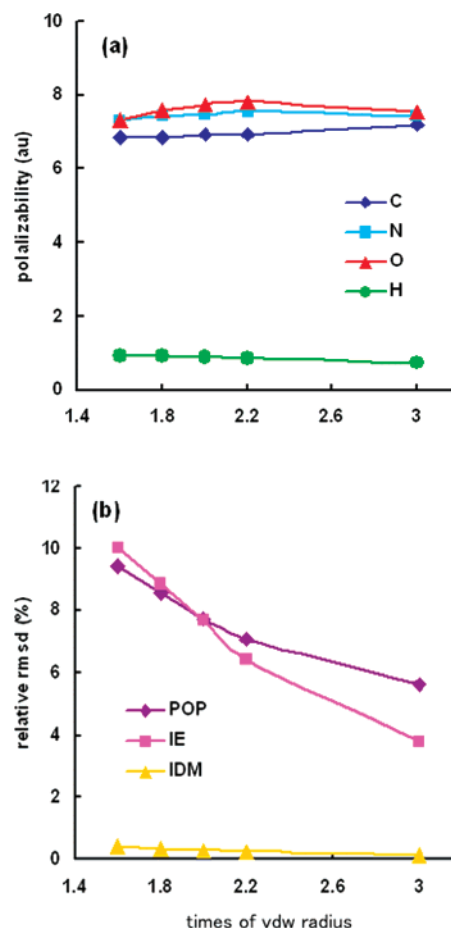


Figure 3. (a) Variation of atomic polarizabilities of guanine for times of van der Waals radius of atoms. (b) Relative root-mean-square deviations of the polarized one-electron potential fitting, induction energies, and induced dipole moments.

were located in the nondamping region. The complete inclusion of 1–3 or more is consistent with Thole's linear model.

Permanent Charge-Induced Dipole Interactions within the Molecule. The intramolecular interactions for permanent charge-induced dipole were studied using model S of guanine. The scaling effect for 1–3, 1–4, and 1–5 or more are shown in Figure 6. The scaling combination of 0.0, 0.5, and 1.0 for 1–3, 1–4, and 1–5 or more were tested. Here, the 1–2 interaction was neglected (zero scaling). The atomic polarizabilities changed greatly by the scaling as shown in Figure 6(a). Even the inclusion of 1–5 or more interaction causes the 30% deterioration of the rms deviation of POP. Because the effect of permanent charges is large, the adjustment of the induced dipoles seems not to be possible. An exclusion of the intramolecular permanent charge-induced dipole interactions is necessary contrary to the case of induced dipole-induced dipole interactions.

Apart from the above effect, an inclusion of the intramolecular permanent charge-induced dipole interaction influences the permanent charges obtained from the ESP optimization. In the ESP optimization process, this can be corrected for by the inclusion of induced dipole moments in addition to the permanent charges.^{16,43} However, the intrinsic deterioration by the intramolecular permanent charge-induced

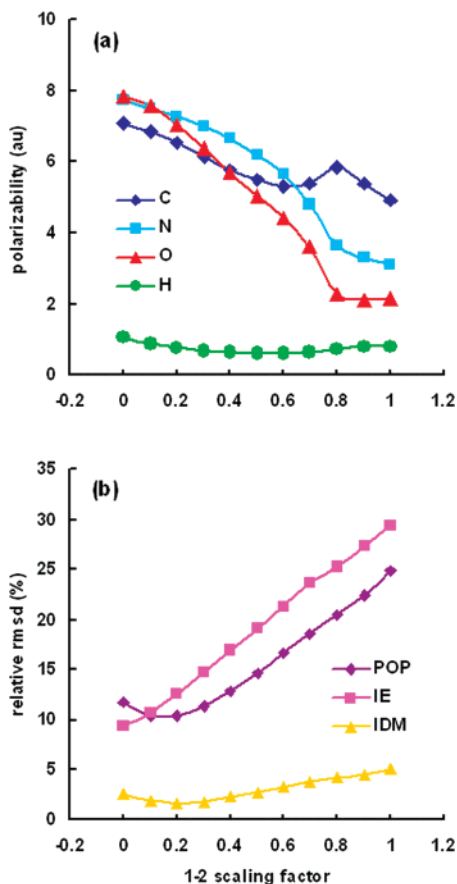


Figure 4. (a) Variation of atomic polarizabilities of guanine by 1-2 bond scaling of simple model. (b) Relative root-mean-square deviations of the polarized one-electron potential fitting, induction energies, and induced dipole moments.

dipole interaction cannot be corrected. Thus, the correction of the permanent charges by the effect of the intramolecular induced dipoles was not executed in our ESP optimization.

Application of Polarization Models for Nucleic Acid Base Interactions. Five types of nucleic acid base complexes were studied: the Watson–Crick adenine–thymine pair (AT-wc), the Hoogsteen adenine–thymine pair (AT-h), the Watson–Crick cytosine–guanine pair (CG-wc), the stacked adenine–thymine pair (AT-s), and the stacked cytosine–guanine pair (AT-s). The optimized geometries and the quantum mechanical interaction energies of the base pairs are taken from the previous work.³⁸ The target interaction energies were calculated by using MP2/6-311++G(3df,2pd) for the hydrogen bond base pairs and by using MP2/6-311++G(2d,2p) for the stacked base complexes. The basis set super position error (BSSE) corrected interaction energies⁴⁵ are shown in Table 4.

The classical energies were estimated by using the polarized model potential function. The atomic charges and van der Waals parameters are taken from our previous work.³⁸ The polarization energies were estimated by using the implicitly interacting model and the explicitly interaction model. The interaction energies and polarization energies of the five nucleic acid complexes are shown in Table 4. For the empirical T1 model in Table 4, the empirical atomic polarizabilities reported by van Duijnen and Swart were

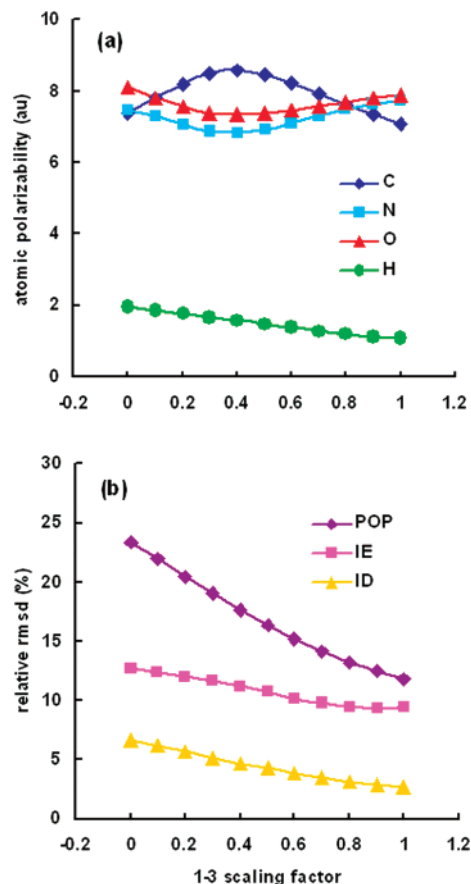


Figure 5. (a) Variations of atomic polarizabilities of guanine by 1-3 bond scaling of simple model. (b) Relative root-mean-square deviations of polarized one-electron potential fitting, induction energies, and induced dipole moments.

used: H 3.0588 au; C 8.7979 au; N 6.6704 au; and O 5.6480 au.²⁸ Model ab, model T1, and model S show quite good results for AT-cw, AT-h, and CG-wc. Model A and the empirical model T1 show slightly too high values for AT-wc and AT-h. Model T2 and the empirical model T1 show similar high polarization energies for CG-wc. The empirical parameters were fitted to the experimental molecular polarizabilities in gas phase. Since the polarizabilities are reduced in the condensed phase, the use of empirical values might have a tendency to overestimate the polarization energy.³⁸ Model b and model D3 show a little too low values. The contribution of the polarization effect is small in the stacked base complexes. All polarization models studied here show similar polarization energies for the stacked complexes.

The dipole moments of the complexes are shown in Table 4. The dipole moment estimated by the electrostatic term of PMP (Ees) shows the state that has not polarized. The dipole moments were relatively well reproduced except for model A applied to the hydrogen bond type base pairs. The relative rms deviations of surface ESP are also shown in Table 4. The relative rms deviations were then less than 12% except for models a, T2, and D3 of CG-wc. The electron distribution change by the formation of the complex as well as the interaction energies is well represented by the implicitly interacting polarizability model and the explicitly interacting polarizability model.

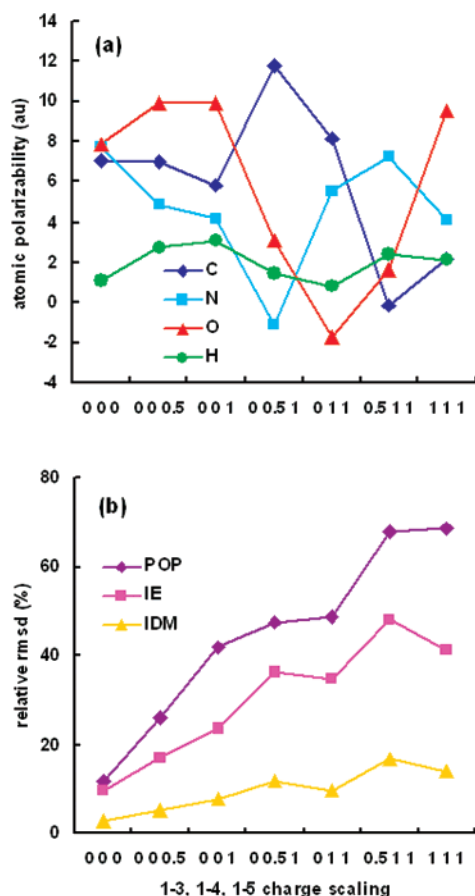


Figure 6. (a) Variations of atomic polarizabilities of guanine by 1-3, 1-4, and 1-5 or more bond scaling for charge-induced dipole interactions. (b) Relative root-mean-square deviations of the polarized one-electron potential fitting, induction energies, and induced dipole moments.

Discussion

The POP optimization is a powerful and practical method to determine multicenter dipole polarizabilities that can be used for determining polarizable force fields. This method can be applied to any molecule that can be calculated by quantum mechanics. A test charge used in POP optimization mimics a nonuniform external field induced by a nearby ion. Since the change in the electron density is a target of the optimization, the higher order multipole contributions in the single-center expansion are all included. It is readily possible to implement this method in both the implicitly interacting and the explicitly interacting polarizability models.

In the implicitly interacting model, the ab model including isotropic atom polarizabilities and anisotropic bond polarizabilities showed good results. The anisotropic contribution is directly calculated by the anisotropic polarizabilities along the chemical bond. On the other hand, the anisotropy is included in the convergence process of the induced dipole–induced dipole interactions in the explicitly interacting model. The explicitly interacting model needs substantially more computer time compared with the implicitly interacting model. The T1 and S models have shown great results at the same level as model ab. Although the treatment of the induced dipoles is quite different from the implicitly interact-

ing model, the polarization anisotropy of molecule is similarly included in the explicitly interacting model.

When the multicenter polarizability parameters of each atom and/or each bond were individually relaxed, we obtained parameters that differed from what can be expected by chemical intuition. In this study, the parameters of each atomic species and/or each bond have been optimized. The rms deviation hardly deteriorated at all though the number of parameters decreased by the restraint to the atomic species and/or the bond species. In the empirical approach by Thole, one polarizability is adopted for each atom irrespective of chemical environment. The empirical atomic polarizabilities of Thole were somewhat different from those determined by the POP optimization, but comparatively good results were obtained in both of the parameter sets for the studied nucleic acid base complexes. In the ESP optimization, the charge restraints for deriving atomic charges have often been introduced in order to obtain transferable parameters for the conformation.³⁴ Although the multicenter polarizabilities are determined for each molecule by using POP optimization and applied in the molecular mechanics calculations, it seems that a small number of transferable polarization parameters can be obtained by the restraint for atomic species especially in the explicitly interacting model as inferred from the empirical approach of Thole.²⁷

When the multicenter polarizabilities of a small molecule are used as segments of a large molecule, it is necessary to exclude the induced dipole–induced dipole interactions within the segment in the implicitly interacting model. This manipulation is somewhat troublesome for the treatment of intrasegment interaction. On the other hand, it is not necessary to exclude this contribution in the explicitly interacting model. Thus, the consistent treatment of inter- and intramolecular polarization is possible in the explicitly interacting model. Especially model S is suitable for polarizable force fields because the complicated damping calculations of exponential type can be avoided.

The electron density change induced by a test charge is reflected purely in the polarized one electron potentials. The polarization by the intramolecular atomic charges is not originally included in the density change itself. Those are included in the atomic charges that are determined by the ESP optimization. When the multicenter polarizabilities of small molecule are used as the segments of a large molecule, it is necessary to exclude the atomic charge-induced dipole interactions within the segment. Thus, the consistent treatment between the intermolecular polarization and intramolecular polarization is difficult for the atomic charge-induced dipole interactions. Ren and Ponder suggested a treatment of the polarization group in which the net charges are small,¹⁸ but such grouping is difficult for the conjugate system such as nucleic acid bases. In the construction of the AMBER polarizable force field (ff02), atomic charges were optimized using the electrostatic potential around a molecule, in which the electrostatic potential, created by the induced dipoles and atomic charges, is subtracted.^{16,43} Such a correction for the double counting of the permanent charge-induced dipole is valid for the estimation of electrostatic energy, but the induction energy is not corrected. In the POP optimization

Table 4. Nucleic Acid Base Interaction Energies in kcal/mol, Dipole Moments in Debye, and rms Deviations of Electrostatic Potentials in kcal/mol

model	damping type	AT-wc				CG-wc				AT-h			
		<i>E</i>	<i>E</i> _{plz}	dipole moment	rmsd ESP	<i>E</i>	<i>E</i> _{plz}	dipole moment	rmsd ESP	<i>E</i>	<i>E</i> _{plz}	dipole moment	rmsd ESP
a		−15.5	−4.4	1.4	1.2 (10) ^b	−28.6	−9.3	6.3	2.5 (16)	−17.5	−4.2	6.3	1.1 (10)
b		−14.7	−3.6	1.4	1.2 (10)	−27.5	−8.2	6.5	1.6 (10)	−16.8	−3.5	6.4	1.3 (12)
ab		−15.5	−4.4	1.2	1.3 (11)	−28.4	−9.1	6.4	1.7 (11)	−17.6	−4.3	6.1	1.3 (12)
A		−17.8	−6.7	2.2	1.3 (11)	−29.1	−9.9	5.4	1.3 (9)	−18.9	−5.6	6.7	1.3 (11)
T1	Exp 1	−16.5	−5.4	1.3	1.1 (10)	−29.6	−10.4	6.3	1.6 (11)	−18.5	−5.2	6.1	1.1 (10)
T1 empirical	Exp 1	−17.4	−6.2	1.4	1.0 (8)	−31.8	−12.5	6.4	1.9 (12)	−19.3	−6.0	6.3	0.9 (8)
T2	Exp 2	−15.8	−4.7	1.8	1.1 (9)	−34.3	−15.1	6.5	2.4 (15)	−17.8	−4.4	6.6	1.0 (9)
D3	1-2,1-3 Exp 3	−14.3	−3.1	1.8	1.2 (10)	−24.8	−5.5	5.7	2.6 (17)	−16.2	−2.9	6.6	1.2 (11)
S	1-2 0.1	−15.2	−4.1	1.3	1.2 (10)	−28.9	−9.6	6.5	1.6 (10)	−17.3	−4	6.2	1.1 (10)
Ees+Evdw		−11.1		2.2	1.3 (11)	−19.3		4.6	2.4 (16)	−13.3		6.8	1.2 (11)
MP2/6-31+G* ^a		−13.8		1.6	0.6 (5)	−27.5		6.1	0.7 (4)	−14.3		6.4	0.6 (5)
MP2/6-311++G(3df,2pd) ^a		−15.7		1.5		−30.0		5.8		−17.5		6.1	

model	damping type	AT-s				CG-s			
		<i>E</i>	<i>E</i> _{plz}	dipole moment	rmsd ESP	<i>E</i>	<i>E</i> _{plz}	dipole moment	rmsd ESP
a		−9.8	−0.6	6.9	1.2 (8)	−10.7	−1.0	4.5	1.5 (9)
b		−9.6	−0.4	6.6	1.1 (8)	−10.6	−0.9	4.3	1.1 (7)
ab		−9.8	−0.6	6.7	0.8 (6)	−10.8	−1.1	4.3	1.0 (7)
A		−9.8	−0.6	6.9	1.2 (8)	−10.5	−0.9	4.2	0.9 (6)
T1	Exp 1	−9.8	−0.5	6.7	0.9 (6)	−10.8	−1.1	4.3	1.1 (7)
T1 empirical	Exp 1	−9.7	−0.5	6.7	0.9 (6)	−10.7	−1.0	4.3	1.1 (7)
T2	Exp 2	−9.7	−0.5	6.8	0.8 (6)	−10.9	−1.2	4.3	1.1 (7)
D3	1-2,1-3 Exp 3	−9.9	−0.7	6.6	0.9 (7)	−10.6	−0.9	4.3	1.2 (8)
S	1-2 0.1	−9.7	−0.5	6.7	0.8 (6)	−10.8	−1.1	4.2	1.0 (6)
Ees+Evdw		−9.2		7.0	1.4 (10)	−9.7		4.7	1.7 (11)
MP2/6-31+G* ^a		−5.4		6.4	0.5 (3)	−8.4		4.1	0.6 (4)
MP2/6-311++G(2d,2p) ^a		−8.4		6.2		−11.4		3.8	

^a The BSSE corrected interaction energies are taken from ref 38. ^b Rrmsd %.

the effect from the atomic charges should be excluded, and the atomic charge-induced dipole interactions within the segment should be excluded as much as possible in the evaluation of the induction energies. Therefore, in the explicitly interacting model the treatment for the intrasegmental atomic charge-induced dipole interaction has a completely different necessity from the treatment for the intrasegmental induced dipole–induced dipole interaction. On the other hand, in the implicitly interacting polarization model both of the intrasegmental interactions must be excluded.

The intermolecular interaction energy can be divided into electrostatic (ES), exchange repulsion (EX), polarization (PL), and charge-transfer (CT) terms in the calculations of HF level.⁴⁷ The dispersion force (DIS) is estimated by the difference between the HF energy and the energy including electron correlation effect. In the polarizable model potential (PMP) function used here a polarization (plz) term is added to an existing pair potential function which consists of an electrostatic (es) term and a van der Waals (vdw) term. The es and plz terms correspond to the ES and PL terms, respectively. The vdw term represents the EX and the DIS. An explicit CT term is not included in the PMP function. However, it is difficult to obtain a one-to-one correspondence

between energies obtained by the quantum and the classical calculations, because the atomic charges and the multicenter polarizabilities were derived in this study from the calculations of the MP2 level that include the effect of electron correlation. In the previous study on methanol using the PMP function, a quite good agreement of the interaction energies had been shown for ion–methanol and methanol–ion–methanol systems.³⁷ The ions of Cl[−], Na⁺, and Mg²⁺ were used in that study. In the ion–methanol complex the energy decomposition results showed that the ES, PL+CT+R, and EX+def+DIS roughly correspond with the es, plz, and vdw of the PMP function, respectively. Here, the PL+CT+R shows the sum of the energies of PL, CT, and the residual. The EX+def+DIS shows the sum of the energies of EX, deformation, and DIS. Recently, Donchev et al. showed that the MP2 correction of ES and EX for DIS works well in the development of their quantum mechanical polarizable force field though the MP2 correction of induction energy for DIS was neglected.⁴⁸ The vdw term (L-J potential) of PMP function shows the EX and DIS. The inclusion of the plz term to the present pair potential may partly double-count the dispersion because the multicenter polarizabilities were derived from the MP2 calculations. In the development of

the PMP function, the parameters of the vdW term are treated as adjustable and lose their original physical meaning.^{37,38}

In the previous study on the nucleic acid bases it was pointed that the multicenter polarizabilities estimated by POP optimization partly include the ability of CT.³⁸ Concerning the CT contribution, Chelli et al. suggested that classical polarizable force fields underpolarize in a hydrogen-bond model system of water.⁴⁹ On the other hand, it has been suggested that the overpolarization occurs in the condensed phase by the neglect of coupling between many-body exchange and polarization.⁵⁰ In the POP optimization the reference quantum mechanical calculations of nucleic acid bases were computed at the MP2/6-31+G* level since the calculated molecular polarizabilities were relatively close to the experimental values in the condensed phase.³⁸ For example, the theoretical and the experimental molecular polarizabilities of guanine are 96.8 au and 91.8 au, respectively. The largest theoretical value reported is 106.7 au.⁴⁶ Since the polarization of the molecule is reduced by the electron repulsion and is increased somewhat by the CT, the choice of MP2/6-31+G* might be adequate for the estimation of polarization energy in the condensed phase.

The present polarizable force fields still have problems and should be investigated further.^{48,51} However, the results from the QM study reproduced the interaction energies and the charge density changes though the same parameters were applied to quite different systems (hydrogen bond base pair, stacked base pair, and ion base complex). Especially, the interactions of the complexes including ions are excellently improved in comparison with the pair potential as shown in the previous work.³⁸ It seems that these results give more encouragement to the development of polarizable force fields.

A systematic development of high quality polarizable force fields is possible by the POP optimization. The development of polarizable force fields for proteins and nucleic acids has already been started by using POP optimization. Our intention is to further elaborate this recipe for the development of polarizable force fields.

Acknowledgment. The authors are grateful to Prof. N. Kosugi of Institute for Molecular Science for his helpful discussions and Prof. M. Yamakawa of Kinjo Gakuin University for his technical support. This work was supported by the Grant-in-Aid for Scientific Research (C) of Japan Society for the Promotion of Science.

References

- (1) Karplus, M. *Acc. Chem. Res.* **2002**, *35*, 321.
- (2) Kollman, P. A.; Massova, I.; Reyes, C.; Kuhn, B.; Huo, S.; Chong, L.; Lee, M.; Lee, T.; Duan, Y.; Wang, W.; Donini, O.; Cieplak, P.; Srinivasan, J.; Case, D. A.; Cheatham, T. E., III *Acc. Chem. Res.* **2000**, *33*, 889.
- (3) Giudice, E.; Lavery, R. *Acc. Chem. Res.* **2002**, *35*, 350.
- (4) Simonson, T.; Archontis, G.; Karplus, M. *Acc. Chem. Res.* **2002**, *35*, 430.
- (5) Saiz, L.; Klein, M. L. *Acc. Chem. Res.* **2002**, *35*, 482.
- (6) Nakagawa, S.; Yu, H.-A.; Karplus, M.; Umeyama, H. *Proteins: Struct., Funct., Genet.* **1993**, *16*, 172.
- (7) Maekawa, K.; Ishikawa, S.; Ishida, H.; Nakagawa, S.; Ohkubo, K.; Yamabe, T. *Mol. Eng.* **1998**, *8*, 9.
- (8) Brooks, B. R.; Bruccoleri, R. E.; Olafson, B. D.; States, D. J.; Swaminathan, S.; Karplus, M. *J. Comput. Chem.* **1983**, *4*, 187.
- (9) Weiner, S. J.; Kollman, P. A.; Case, D. A.; Singh, U. C.; Chio, C.; Alagona, G.; Profeta, S., Jr.; Weiner, P. *J. Am. Chem. Soc.* **1984**, *106*, 765.
- (10) Jorgensen, W. L.; Tirado-Rives, J. *J. Am. Chem. Soc.* **1988**, *110*, 1657.
- (11) MacKerell, A. D., Jr.; Wiórkiewicz-Kuczera, J.; Karplus, M. *J. Am. Chem. Soc.* **1995**, *117*, 11946.
- (12) Singh, U. C.; Kollman, P. A. *J. Comput. Chem.* **1986**, *7*, 718.
- (13) Field, M. J.; Bash, P. A.; Karplus, M. *J. Comput. Chem.* **1990**, *11*, 700.
- (14) Svensson, M.; Humbel, S.; Froese, R. D. J.; Matsubara, T.; Sieber, S.; Morokuma, K. *J. Phys. Chem.* **1996**, *100*, 19357.
- (15) Halgren, T. A.; Damm, W. *Curr. Opin. Struct. Biol.* **2001**, *11*, 236.
- (16) Cieplak, P.; Caldwell, J.; Kollman, P. *J. Comput. Chem.* **2001**, *22*, 1048.
- (17) Wang, Z.-X.; Zhang, W.; Wu, C.; Lei, H.; Cieplak, P.; Duan, Y. *J. Comput. Chem.* **2006**, *27*, 781.
- (18) Ren, P.; Ponder, J. W. *J. Comput. Chem.* **2002**, *23*, 1497.
- (19) Ren, P.; Ponder, J. W. *J. Phys. Chem. B* **2003**, *107*, 5933.
- (20) Kaminski, G. A.; Stern, H. A.; Berne, B. J.; Friesner, R. A.; Cao, Y. X.; Murphy, R. B.; Zhou, R.; Halgren, T. A. *J. Comput. Chem.* **2002**, *23*, 1515.
- (21) Harder, E.; Kim, B.; Friesner, R. A.; Berne, B. J. *J. Chem. Theory Comput.* **2005**, *1*, 169.
- (22) Patel, S.; Mackerell, A. D., Jr.; Brooks, C. L., III *J. Comput. Chem.* **2004**, *25*, 1504.
- (23) Anisimov, V. M.; Lamoureux, G.; Vorobyov, I. V.; Huang, N.; Roux, B.; MacKerell, A. D., Jr. *J. Chem. Theory Comput.* **2005**, *1*, 153.
- (24) Gresh, N.; Šponer, J. E.; Špačková, N.; Leszczynski, J.; Šponer, J. *J. Phys. Chem. B* **2003**, *107*, 8669.
- (25) Chipot, C.; Ángyán, J. G. *New J. Chem.* **2005**, *29*, 411.
- (26) Applequist, J.; Carl, J. R.; Fung, K.-K. *J. Am. Chem. Soc.* **1972**, *94*, 2952.
- (27) Thole, B. T. *Chem. Phys.* **1981**, *59*, 341.
- (28) van Duijnen, P. Th.; Swart, M. *J. Phys. Chem. A* **1998**, *102*, 2399.
- (29) Miller, K. J. *J. Am. Chem. Soc.* **1990**, *112*, 8543.
- (30) Stone, A. J. *Mol. Phys.* **1985**, *56*, 1065.
- (31) Jansen, G.; Hättig, C.; Hess, B. A.; Ángyán, J. G. *Mol. Phys.* **1996**, *88*, 69.
- (32) Garmer, D. R.; Stevens, W. J. *J. Phys. Chem.* **1989**, *93*, 8263.
- (33) Nakagawa, S.; Kosugi, N. *Chem. Phys. Lett.* **1993**, *210*, 180.
- (34) Bayly, C. I.; Cieplak, P.; Cornell, W. D.; Kollman, P. A. *J. Phys. Chem.* **1993**, *97*, 10269.
- (35) Nakagawa, S. *Chem. Phys. Lett.* **1995**, *246*, 256.
- (36) Nakagawa, S. *Chem. Phys. Lett.* **1997**, *278*, 272.
- (37) Nakagawa, S. *J. Phys. Chem. A* **2000**, *104*, 5281.

- (38) Nakagawa, S. *J. Comput. Chem.* **2007**, 28, 1538.
- (39) Ángyán, J. G.; Chipot, C.; Dehez, F.; Hättig, C.; Jansen, G.; Millot, C. *J. Comput. Chem.* **2003**, 24, 997.
- (40) Fletcher, R. *Practical methods of optimization*; Wiley: New York, 1980; Vol. 1, p 10276.
- (41) Møller, C.; Plesset, M. S. *Phys. Rev.* **1934**, 46, 618.
- (42) Hehre, W. J.; Radom, L.; Schleyer, P. v. R.; Pople, J. A. *Ab Initio Molecular Orbital Theory*; Wiley: New York, 1986.
- (43) Frisch, M. J.; Trucks, G. W.; Schlegel, H. B.; Scuseria, G. E.; Robb, M. A.; Cheeseman, J. R.; Montgomery, J. A., Jr.; Vreven, T.; Kudin, K. N.; Burant, J. C.; Millam, J. M.; Iyengar, S. S.; Tomasi, J.; Barone, V.; Mennucci, B.; Cossi, M.; Scalmani, G.; Rega, N.; Petersson, G. A.; Nakatsuji, H.; Hada, M.; Ehara, M.; Toyota, K.; Fukuda, R.; Hasegawa, J.; Ishida, M.; Nakajima, T.; Honda, Y.; Kitao, O.; Nakai, H.; Klene, M.; Li, X.; Knox, J. E.; Hratchian, H. P.; Cross, B.; Adamo, C.; Jaramillo, J.; Gomperts, R.; Stratmann, R. E.; Morokuma, K.; Voth, G. A.; Salvador, P.; Dannenberg, J. J.; Zakrzewski, V. G.; Dapprich, S.; Daniels, A. D.; Strain, M. C.; Farkas, O.; Rabuck, A. D.; Raghavachari, K.; Foresman, J.B.; Cui, Q.; Baboul, A. G.; Clifford, S.; Cioslowski, J.; Stefanov, B. B.; Liu, G.; Liashenko, A.; Piskorz, P.; Komaromi, I.; Martin, R. L.; Fox, D. J.; Keith, T.; Al-Laham, M. A.; Peng, C. Y.; Nanayakkara, A.; Challacombe, M.; Gill, P. M. W.; Johnson, B. G.; Chen, W.; Wong, M. W.; Gonzalez, C.; Pople, J. A. *Gaussian 03 (Revision A.1)*; Gaussian, Inc.: Pittsburgh, PA, 2003.
- (44) Winn, P. J.; Ferenczy, G. G.; Reynolds, C. A. *J. Comput. Chem.* **1999**, 20, 704.
- (45) Boys, S. F.; Bernardi, F. *Mol. Phys.* **1970**, 19, 553.
- (46) Jasien, P. G.; Fitzgerald, G. *J. Chem. Phys.* **1990**, 93, 2554.
- (47) Kitaura, K.; Morokuma, K. *Int. J. Quantum Chem.* **1976**, 10, 325.
- (48) Donchev, A. G.; Galkin, N. G.; Pereyaslavets, L. B.; Tarasov, V. I. *J. Chem. Phys.* **2006**, 125, 244107.
- (49) Chelli, R.; Schettino, V.; Procacci, P. *J. Chem. Phys.* **2005**, 122, 234107.
- (50) Giese, T. J.; York, D. M. *J. Chem. Phys.* **2004**, 120, 9903.
- (51) Engkvist, O.; Åstrand, P.-O.; Karlström, G. *J. Phys. Chem.* **1996**, 100, 6950.

CT700132W